Template Effect Where 1-3 Molecules Drive Formation of a Trimer Carceplex

Darren A. Makeiff and John C. Sherman*[a]

Abstract: The template effect in the formation of a trimer carceplex using 1-3 molecules as templates is explored. Thirteen different templates were studied and template ratios were measured for templates of like and unlike molecularity. Five transition-state models were studied for their binding abilities to see if these mirror the template ratios. The chemical shifts of the guests and the thermodynamic and kinetic values for templation suggest that binding is key, often tight, and that the guest determining step is formation of the last covalent bond. The molecular dynamics of guests as well as the conformational dynamics of both hosts and guests further addresses nature of the recognition between host and guest. Finally, we were surprised to discover that water can bind reversibly to the trimer carceplexes, which will have ramifications to any inner phase reactions conducted inside the cage.

Keywords: carceplex · host–guest systems · molecular recognition · supramolecular chemistry · template synthesis

Introduction

The creation of container compounds has fascinated chemists for a number of years.[1] Approaches vary widely, from use of vesicles to zeolites, from fullerenes to clathrates, from nanotubes to carceplexes. In the case of fullerenes, often only single atoms can be entrapped,[2] whereas in the case of nanotubes or micelles, entire fluids can be contained.[3] Containment lifetime can vary from rapid exchange with the surrounding environment, as is the case with most ordinary complexes, to permanent entrapment where only rupture of covalent bonds can release guests, as is the case with carceplexes.[1] Such permanent containment facilitates characterization of the products. Moreover, the templated assembly process responsible for forming a permanent container can be assessed quantitatively because the template is caught forever in the cage; simple competition experiments render the relative templating abilities of different guests. We have studied template effects involving carceplexes and hemicarceplexes where single molecules have acted as templates.[4] Can multiple molecules act as templates?

Containment of multiple molecules has been demonstrated by several groups. In most cases, guests are readily released by the host. Two arenes have been reversibly bound in Rebek's softballs,[5] as have Diels–Alder reactants.[6] Rebek has also shown similar sized pairs can be bound in dimers of cavitand vases.[7] Fujita has bound pairs of *cis*-stilbene and related species in pyridyl–metal ligating assemblies,[8] sodium adamantane carboxylate in a similar host,[9] and six molecules of *cis*-stilbene in a large metal–ligand cage.[10] Atwood and others have reported non-covalent hexameric resorcinarenes, one of which may contain 18 molecules of methanol.[11] More long-term containment of multiple guests has been reported by Cram in the entrapment of two acetonitriles and two methanols in a sulfide-bridged carceplex,[12] as well as two acetonitriles in a hemicarceplex.[13] We have reported entrapment of two molecules of DMF in a disulfide-linked [5]carceplex,[14] and three molecules of DMF in a trimer carceplex, **5**·$(DMF)_3$ (Scheme 1).[15] We have chosen the latter carceplex for the present study to explore the template effect of multiple molecules as templates. The rigidity of the

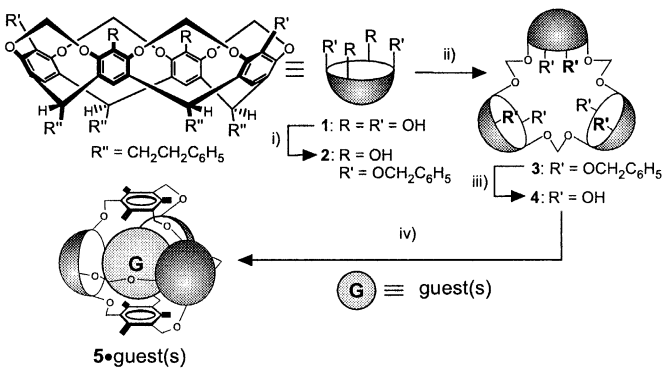

Scheme 1. Synthesis of trimer carceplex **5**·guest(s). i) DBU, BnBr, acetone, 13%; ii) K_2CO_3, CH_2BrCl, DMSO, 42%; iii) H_2, Pd/C, 90%; iv) K_2CO_3, KI, 2,4,6-tris-(bromomethyl)mesitylene, guest(s), 10–35%.

[a] Prof. J. C. Sherman, D. A. Makeiff
Department of Chemistry
2036 Main Mall, University of British Columbia
Vancouver, BC V6T 1Z1 (Canada)
Fax: (+1) 604-822-2847
E-mail: sherman@chem.ubc.ca

Supporting information for this article (all experimental details including syntheses and EXSY experiments) is available on the WWW under http://www.chemeurj.org/ or from the author.

 DOI: 10.1002/chem.200304780

precursors of **5** allow transition-state models to be generated that can bind guests. We found some surprises regarding the mobility of bound guests and the entry and egress of water into the trimer carceplexes. We present here our first exploration of multiple molecules as templates, including the binding and dynamics of various trimer complexes.

Results and Discussion

Synthesis: The synthesis of trimer carceplex **5**·guest(s) was achieved by the procedure described previously,[15] except that optimization of the key reactions (**1**→**2**, **2**→**3**) enhanced the overall yields by over tenfold (see Supporting Information for modified preparations). The final step (**4**→**5**) was originally reported in DMF as solvent, and gave **5**·$(DMF)_3$. Presently we found that neat solvents furnished **5**·butyrophenone, **5**·$(DMA)_2$,[16] **5**·$(DMSO)_3$, **5**·$(NMP)_2$, and **5**·NFP mixed with **5**·$(NFP)_2$, typically in yields in excess of 35%.[17] A more general solvent was sought to expand the template studies to non-solvent guests/templates. The ideal solvent is one that is suitably polar for the reaction but is itself a poor template. We settled on *N*-formylpiperidine (NFP = **10**), a poor though suitable template. Thus five additional carceplexes containing guests **6**–**9** and **12** were generated. Mixed carceplexes **5**·DMSO·NFP and **5**·4-ethylacetophenone·NFP were also

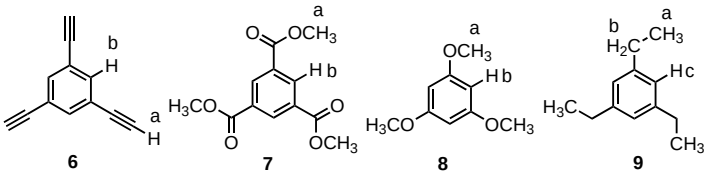

obtained using NFP as solvent and DMSO and 4-ethylacetophenone, respectively, as guests. Carceplexes **5**·acetophenone·NFP and **5**·propiophenone·NFP were obtained likewise, but only as inseparable mixtures with both **5**·NFP and **5**·$(NFP)_2$. Valerophenone and heptanophenone as guests gave poor yields of carceplex mixtures and were not pursued further. To explore the effect of a larger pored carceplex, we prepared the methyl-less capped **13**·guest(s), where guests are **6** (60%), **11** (22%), $(DMA)_2$ (81%), and $(DMF)_3$ (40%), by capping with 1,3,5-tris(bromomethyl)benzene instead of 2,4,6-tris(bromomethyl)mesitylene.

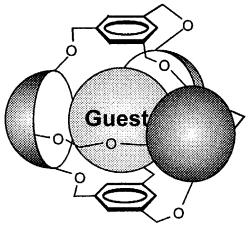

13·guest(s)

Potential transition-state models were prepared as follows. Trimers **3** and **4** were prepared as described above. Tris-hydroxy trimer cavitand **14** was isolated as a by-product in the synthesis of carceplex **5**·$(DMF)_3$,[16] and optimized to 20% yield; it was also prepared in 25% yield via partial removal of the caps of **5**·$(DMF)_3$ by treatment with TFA. Tris-benzyl trimer cavitand **15** was obtained in 56% yield by benzylation of **14**. Tris-4-cyanobenzyl trimer cavitand **16** was obtained in 24% yield by the corresponding cyanobenzylation of **14**. Finally, *m*-xylyl-capped trimer cavitand **17** was obtained by capping **14** with α,α'-dibromo-*m*-xylene in a one-pot reaction starting from trimer **4** in 19% yield. Owing to their cookie jar shape, we will refer to these hosts as trimer cavitands (not to be confused with simple single cavitands).

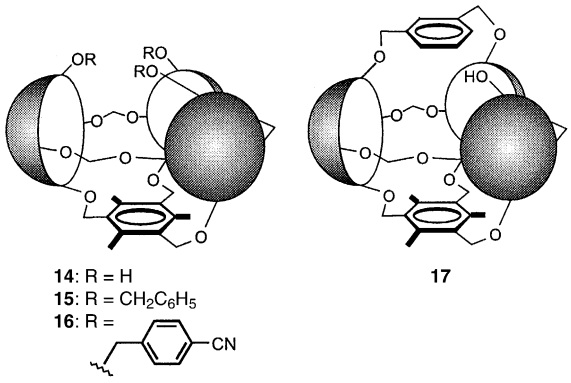

Template studies: This is the first report of template ratios for templates other than single molecules, so the equations used for their calculations need to be generated.[4] We use TR_{xy} to denote a template ratio between *x* and *y* molecules, where *x* and *y* are integers. Thus template ratios between two single molecules, TR_{11}, are obtained from product ratios (by integration of ^1H NMR signals) from competition reactions and starting ratios of the two guests/templates (which are in excess of host), using Equation (1).

$$TR_{11} = \frac{[\mathbf{5}\cdot G_A]\,[G_B]}{[\mathbf{5}\cdot G_B]\,[G_A]} = \frac{K_A k_A}{K_B k_B} \quad (1)$$

where the two single guests are G_A and G_B, K_Z (Z = A or B) is the equilibrium constant for formation of the intermediate immediately prior to the guest determining step (GDS) in the presence of guest Z, and k_Z is the rate constant for the GDS starting from said intermediate in the presence of guest Z. A template ratio of *n* for guest A means that the GDS is *n* times faster in the presence of guest A than in the presence of guest B. Tables of template ratios contain more than two templates; the poorest template is usually set to 1.

Note that TR_{11} are unitless. Likewise for any template ratio between templates of like molecularity, TR_{xx}. However, when the templates have different molecularity the template ratio, TR_{xy}, will contain units. For example, TR_{12} will have units of M according to Equation (2).

$$TR_{12} = \frac{[\mathbf{5}\cdot G_A]\,[G_B]}{[\mathbf{5}\cdot G_A\cdot G_B]} = \frac{K_A k_A}{K_{AB} k_{AB}} \quad (2)$$

where in this case the single molecule template is guest A, and the two molecule template is guest A and guest B. Qualitatively, a larger TR_{12} means that the single molecule is a better

template than the two molecule pair. One can also express a TR_{21}, where the opposite is true ($TR_{21} = 1/TR_{12}$). An analogy to effective molarities can be made such that a TR_{12} of n means that an effective molarity of n M in guest B is needed for $G_A \cdot G_B$ to equal the templating power of G_A alone. In the case of an A, B, C system, where the single molecule template is guest C, and the two molecule template is A and B, the units are still M ($TR_{12} = [\mathbf{5} \cdot G_C][G_B][G_A]/[\mathbf{5} \cdot G_A G_B][G_C]$). Analogously in this case, a TR_{12} of n means that an effective molarity of n M in guest B (or A) is needed for $G_A \cdot G_B$ to equal the templating power of G_C alone. Analogous equations and analyses can be made for other template ratios, TR_{xy}.

Table 1 lists single molecule versus single molecule template ratios (TR_{11}) for forming **5**·guest determined at ambient temperature and at 70 °C, all normalized to the weakest guest. Table 2 lists two molecule versus two molecule template ratios (TR_{22}) for forming **5**·NFP·arylketone normalized to the weakest guest. Table 3 lists single molecule versus two molecule template ratios (TR_{12} and TR_{21}) for forming **5**·guest(s) for the following sets of templates: **8**:NFP·4-ethylacetophenone, **12**:NFP·4-ethylacetophenone, NFP:NFP·4-ethylacetophenone, NFP:NFP·acetophenone, and NFP:NFP·propiophenone. Table 4 lists template ratios (TR_{22}, TR_{23}, and TR_{33}) for forming **5**·guests for six sets of multiple molecule templates. Table 5 lists single versus three molecule template ratios (TR_{13} and TR_{31}). Table 6 lists template ratios at different temperatures for the three pairs of templates: **6**:$(DMSO)_3$ (TR_{13}), **6**:NFP·DMSO (TR_{12}), and NFP·DMSO:$(DMSO)_3$ (TR_{23}). Finally, Table 7 lists the thermodynamic and kinetic values for template ratios (TR_{13}, TR_{12}, and TR_{23}) derived from van't Hoff plots of the data from Table 6. Since template ratios contain both equilibrium constants and rate constants, and since template ratios represent differences between two sets of templates, the van't Hoff plots yield $\Delta\Delta H^\circ + \Delta\Delta H^\ddagger$ from the slope, and $\Delta\Delta S^\circ + \Delta\Delta S^\ddagger$ from the y intercept.

To facilitate interpretation of the template ratio data, it is instructive to examine the chemical shifts of some of the

Table 1. Template ratios (TR_{11}) in the formation of **5**·guest from single-molecule templates.

Guest	Template ratio TR_{11}[a] RT	70 °C	
1,3,5-triethynylbenzene (**6**)	860	11000	(440)
trimethyl 1,3,5-benzene tricarboxylate (**7**)	55	280	(11)
1,3,5-trimethoxybenzene (**8**)	25	260	(10)
1,3,5-triethylbenzene (**9**)	23	–	
hexanophenone (**12**)	5	50	(2)
butyrophenone (**11**)	1	25	(1)
1-formylpiperidine (**10**)	–	1	

[a] Values in brackets are relative to butyrophenone. RT = room temperature.

Table 2. Template ratios (TR_{22}) for **5**·(NFP·guest).

Guest	TR_{22}
4-ethylacetophenone	15
acetophenone	2
propiophenone	1

Table 3. Template ratios TR_{12} and TR_{21} for single molecules (G) versus NFP·aryl ketone (NFP·G_B) at 70 °C.

G	G_B	TR_{12} (G:NFP·G_B)[a] [M]	TR_{21}[b] (NFP·G_B:G) [M^{-1}]
8	4-ethylacetophenone	2.4 (280)	0.42
12	4-ethylacetophenone	0.32 (40)	3.1
NFP	4-ethylacetophenone	0.0087 (1)	110 (16)
NFP	acetophenone	0.059	17 (2)
NFP	propiophenone	0.15	7 (1)

[a] Normalized values relative to TR_{12} (NFP:NFP·4-ethylacetophenone) are given in brackets. [b] Normalized values relative to TR_{21} (NFP·propiophenone:NFP) are given in brackets.

Table 4. Template ratios (TR_{22}, TR_{23}, TR_{33}) for multiple-molecule templates in the formation of **5**·guests.

Solvent mixture (v/v)	Guest A (G_A)	Guest B (G_B)	TR_{22} (G_A:G_B)	TR_{23}/M (G_A:G_B)	TR_{33} (G_A:G_B)
DMSO:DMF (1:9)	$(DMSO)_3$	$(DMF)_3$	–	–	480
DMA:DMSO (9:1)	$(DMA)_2$	$(DMSO)_3$	–	0.17	–
DMA:DMSO (8:2)	$(DMA)_2$	$(DMSO)_3$	–	0.17	–
DMA:DMF (3:7)	$(DMA)_2$	$(DMF)_3$	–	11	–
DMA:DMF (1:1)	$(DMA)_2$	$(DMF)_3$	–	15	–
DMA:NMP (1:1)	$(DMA)_2$	$(NMP)_2$	1.1	–	–

Table 5. Template ratios (TR_{13} and TR_{31}) for forming **5**·guest(s) using $(DMSO)_3$ and $(DMF)_3$ against tris-acetylene **6**.

Guest A(G_A)	Guest B(G_B)	Solvent	TR_{13}(G_A:G_B)	$TR_{31} \times 10^3$(G_B:G_A)
6[a]	$(DMF)_3$	DMSO/DMF 1:9	490000 M^2	0.02 M^{-2}
6[a]	$(DMSO)_3$	DMSO/DMF 1:9	1100 M^2	0.91 M^{-2}
6[b]	$(DMSO)_3$	DMSO/NFP 1:10	43 M^2	23 M^{-2}

[a] [**6**] = 28.2 mM. [b] [**6**] = 6.54 mM.

Table 6. Temperature dependence of template ratios for forming **5**·guest(s) for the three pairs: **6**:$(DMSO)_3$ (TR_{13}), **6**:NFP·DMSO (TR_{12}), and NFP·DMSO:$(DMSO)_3$ (TR_{23}).

T [°C][a]	TR_{13} [M^2]	TR_{12} [M]	TR_{23} [M]
30	51	2300	0.022
40	97	3100	0.032
50	210	3900	0.058

[a] Temperature fluctuation: ± 1.0 °C over the course of the reaction. [NFP] = 8.62 M, [DMSO] = 607 mM, [**6**] = 8.91 mM.

Table 7. Thermodynamic/kinetic values for template ratios for forming **5**·guest(s) using the three pairs: **6**:$(DMSO)_3$ (TR_{13}), **6**:NFP·DMSO (TR_{12}), and NFP·DMSO:$(DMSO)_3$ (TR_{23}).

	$\Delta\Delta H^\circ + \Delta\Delta H^\ddagger$ [kcal mol^{-1}]	$\Delta\Delta S^\circ + \Delta\Delta S^\ddagger$ [cal mol^{-1} K]	$T(\Delta\Delta S^\circ + \Delta\Delta S^\ddagger)$ [kcal mol^{-1}][a]	$\Delta\Delta G^\circ + \Delta\Delta G^\ddagger$ [kcal mol^{-1}][a]
TR_{13}	-14 ± 2	54 ± 5	16 ± 2	-30 ± 4
TR_{12}	-5.3 ± 0.1	32.7 ± 0.2	9.7 ± 0.1	-15.0 ± 0.2
TR_{23}	-9 ± 2	24 ± 2	7.1 ± 0.6	-16 ± 3

[a] T = 298 K.

entrapped guests (Table 8). It is evident from the $\Delta\delta$ that the substituents on the 1,3,5-trisubstituted arenes are oriented into the bowls, the greatest shielding region of the host. These guests appear to be the best templates, which is consistent with the complementarity of the symmetry (C_3 axis) of these guests to that of the host. The ^{1}H NMR data, in combination with examination of CPK models and modeling using MM2 calculations (Figure 1) suggest that these molecules have the best van der Waals contacts, with tris-acetylene **6** having the best fit of all. Smaller guests (**10**, **11**, and **12**) have less van der Waals contacts than **6**, while larger guests **7** have repulsive interactions with the host. Guests **8** and **9** are only slightly larger than **6**, but the "elbow" of their XCH_3 groups causes repulsive interactions between their arenes and the intra-bowl acetal bridges. Note that the larger and tighter fitting guests, **6** and **7**, have the largest $\Delta\delta$ values.

Table 8. ^{1}H NMR chemical shifts (sieve-dried $CDCl_3$) for various 1,3,5-trisubstituted benzene derivative guests in **5**·guest. See structures for proton labels.

Guest	Proton	δ_{free} [ppm]	δ_{bound} [ppm]	$\Delta\delta$ [ppm]
trimethyl ester **7**	H_a	3.96	−0.58	4.54
	H_b	8.85	≈7.24[a]	≈1.61
tris-acetylene **6**	H_a	3.08	−1.24	4.32
	H_b	7.55	5.91	1.64
	H_a	1.23	−2.03	3.26
triethyl **9**	H_b	2.60	0.78	1.82
	H_c	6.86	5.12	1.74
trimethoxy **8**	H_a	3.75	0.53	3.22
	H_b	6.08	4.34	1.74

[a] Signal is hidden under ArH protons of the carceplex feet.

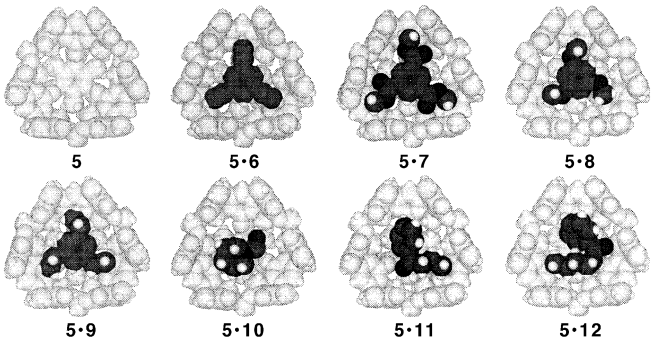

Figure 1. MM2 minimized structures of carceplexes **5**·guest. To simplify calculations, the pendent groups $CH_2CH_2C_6H_5$ of the [4]cavitand subunits were replaced with hydrogen atoms. For clarity, the mesityl caps and parts of the arenes have been removed to show the geometries of each entrapped guest inside the host.

The temperature effect on the template ratios for the single molecule templates with respect to each other is small; a temperature increase of 45 °C yields a decrease in selectivity by a factor of two in most cases, and by a factor of five for **7**. Such a small effect is expected amongst like molecularity templates. Guest **7** may have more conformational constraint upon binding than the other guests (see below), and thus a greater entropic cost upon binding.

Regarding the two-molecule guests from Tables 2 and 3, NFP·4-ethylacetophenone is best, likely due to superior van der Waals contacts. The ethyl group can position its methyl into a bowl, which has been shown to be a favorable interaction.[4, 18] In addition, NMR data and models suggest that 4-ethylacetophenone can span two bowls, while acetophenone and propiophenone cannot. NFP occupies the third bowl. It is difficult to say how important the interactions are between these three aryl ketone guests and their respective cohabiting NFP.

Regarding the three-molecule templates (Tables 4 and 5), DMSO is far better than DMF. This was also observed in the case of the prototypical carceplex, which contained one molecule as template.[4] So it may be a matter of better host–guest contacts, with DMSO having more electron deficient methyls, which interact more strongly with the π-electron rich bowls. Guest–guest interactions may also play a role. Again, this is difficult to assess. Another factor in all cases is the desolvation energy of the guest in the given solvent.[19] Although in cases here (see below) and elsewhere we have shown that change of solvent does not have a substantial impact on the template effect,[20] it is evident from Table 5 that solvent is important: TR_{13} for **6**:$(DMSO)_3$ is 26 times greater in DMF than in NFP. This is likely a reflection of the better solvation of the polar DMSO in the more polar DMF.

From Tables 6 and 7 it is evident that lower molecularity templates are entropically favored: higher molecularity templates are weaker at higher temperatures where the greater entropic cost of collecting several molecules is exacerbated. It is also clear that the lower molecularity templates are enthalpically favored. One might expect the group of smaller molecules to manifest better van der Waals interactions, as they can better fill the nooks and crannies of the cavity. This may be the case in larger systems, but it is clearly not the case for this trimer carceplex with this small set of few guests. Again, the enthalpic interaction between guests with multi-molecule templates is difficult to assess.

Transition-state models: In previous template work, we sought transition-state models to probe the driving forces for the template effect.[20] Recognition upon binding was shown to be the dominant factor, as thermodynamic selectivity of guest binding to transition-state models mirrored the kinetic template ratios.[20] Is this the case with the trimer carceplex? The trimer system differs from previous systems in a number of ways. The trimer precursor **4** is itself a preorganized host with a well-defined surrounding cavity, whereas the two bowl carceplexes and hemicarceplexes start from single cavitands, which have small and very open cavities.[4, 21] Likewise, once the trimer is capped on one side (e.g., **14**–**17**), there is a fairly large cavity, but a single small entrance. At the transition state, there may be a need for guest departure before a second guest can enter. Finally, more than one guest is involved in some cases. We attempt to address some of these issues below.

The simplest transition-state models, both synthetically and structurally, are trimers **3** and **4**. These hosts are moderately rigid and contain enforced cavities similar in size and shape to that of carcerand **5**. They both have two relatively large

openings at opposite sides of the host, so entrance and egress of guests could be concerted. Based on the above results, the best template, tris-acetylene **6**, was added to solutions of hexabenzyl **3** or hexahydroxy **4** in various solvents. Complexes were observed that manifest slow exchange on the ^{1}H NMR timescale. Stability constants were readily determined via integration of the bound and free host and guest signals (Table 9). Hexabenzyl **3** is clearly a stronger binder in [D_5]nitrobenzene, but not in $CDCl_3/CD_3OD$ (19:1) (solubility limited comparison to these two solvent conditions). Hexahydroxy **4** aggregates in [D_5]nitrobenzene, whereas hexabenzyl **3** appears to be monomeric. Although guest binding appears to break up the aggregate of **4**, binding is still weak. The hydroxyl groups may bind to the nitrobenzene solvent and enhance its competitiveness as a guest. The benzyl groups of **3** may provide additional favorable interactions with the tris-acetylene guest. Along these lines, the bound guest signals appears at -0.32 in **3**, but at -0.13 for **4** in [D_5]nitrobenzene, which suggests tighter binding with **3**. Other solvents (Table 9) compete with the guest more effectively for the cavity of **3**. This is not the case for **4**, where methanol likely binds to the hydroxyl groups of **4** and may provide additional interactions with the guest.

Table 9. Stability constants (K_s) for complexes **3·6** and **4·6** in various deuterated solvents.[a]

Solvent	K_s [M^{-1}] **3·6** (R = OBn)	**4·6** (R = OH)
[D_5]nitrobenzene	35000*	41
[D_8]toluene	1300	–
CD_2Cl_2	180	–
C_6D_6	120	–
$CDCl_3/CD_3OD$ (19:1)	15	190
$CDCl_3$	13	–

[a] Error is estimated to be ± 10%. [*] Could not be measured directly: determined from $K_{rel}[(\mathbf{3\cdot6})/(\mathbf{3\cdot7})] \times K_s(\mathbf{3\cdot7})$; see Table 10.

Taking host **3** and [D_5]nitrobenzene as the best combination for binding, other templates were examined (Table 10). A plot of the ln(TR) versus ln(K_S) for guests **6**–**9** gave a correlation of $r^2 = 0.84$. This demonstrates that hexabenzyl trimer **3** in [D_5]nitrobenzene is a reasonable transition-state model for formation of trimer carceplex **5**·guest in NFP.

Table 10. Stability constants (K_s) for **3**·guest ([D_5]nitrobenzene, 300 K).

Guest	K_s [M^{-1}]	TR_{11}*
1,3,5-tris(ethynyl)benzene (**6**)	35000	860
1,3-dimethylphthalate (**18**)	1100	–
1,3,5-triethylbenzene (**9**)	460	23
trimethyl 1,3,5-benzenetricarboxylate (**7**)	100	55
1,3,5-trimethoxybenzene (**8**)	45	25

[*] TR_{11} determined at room temperature in NFP solvent.

One of the goals of using transition-state models is to develop a screen such that potential templates can be found by simple and efficient reversible binding. Thus, in addition to known templates, we explored the binding of new guests to **3**. One guest, 1,3-dimethylphthalate (**18**), bound strongly (Table 10). Seven guests (**19**–**25**) that did not appear to bind to hexabenzyl **3** in [D_5]nitrobenzene at 300 K are shown below. Guests **21**–**23** are likely too small to bind effectively. Benzophenone (**25**) has poor complementarity according to

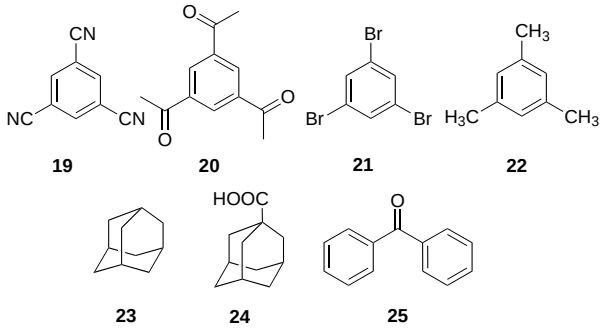

CPK models, as does tris-acetyl **20**, where the carbonyls may have repulsive interactions with the bowl arenes. Acid **24** may be too polar, and tris-nitrile **19** may be electronically non-complementary as the electron rich nitrogens would stick unfavorably into the electron rich bowls. Interestingly, bis-ester **18** binds ten times more strongly than tris-ester **7**. It is likely that **7** is too large, as reflected by its restricted mobility with the carceplex (see below).

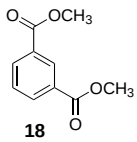

With the above results, we sought potentially superior transition-state models. Thus, trimer **4** was capped with one cap, and the remaining three hyroxyls were left alone (**14**), benzylated (**15**), cyanobenzylated (**16**), and capped with a xylyl group (**17**); the syntheses of which were described above. These new hosts have only one portal, and they have more cavity surface area and are more rigid than **3** and **4**. Thus hosts **14**–**17** may better represent the transition state in forming **5**. Trimer cavitands **14**–**17** manifest unusual conformations, which are worth presentation before their complexation properties can be discussed. The inter-bowl acetal protons are diastereotopic and thus non-equivalent in the ^{1}H NMR spectra. The dispersion of these signals and their chemical shifts give an indication of the conformation of the host. The conformation in all cases is an averaged conformation, as only one species is ever observed. The four extremes are represented in Figure 2. The acetal hydrogens can stick away from the cavity **A**, into the cavity **B**, or one partly into and one partly away from the cavity with both hydrogens pointing away from **C** or toward **D** the cap. No NOE signals were observed between these acetal protons and

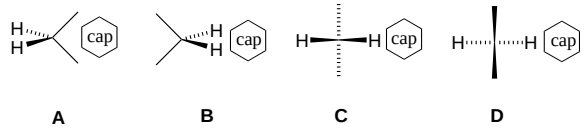

Figure 2. Conformations of trimer cavitands. In each case, the cavity is to the right and the cap is on the bottom. Only one of the three inter-bowl acetals is shown in each case.

the protons of the caps in any case, so conformation **D** can be ruled out as a substantive contributor. In the case of conformation **A**, the chemical shifts will be shifted downfield ($< \approx 5.5$ ppm) and dispersion should be low (< 0.2 ppm). Conformation **B** should manifest upfield chemical shifts ($> \approx 5.7$ ppm) and low dispersion, and **C** should manifest moderate shifts and high dispersion (> 0.5 ppm). Conformations **B** and **C** would be difficult to distinguish based solely on chemical shifts and dispersion. Table 11 lists the relevant data for trimer cavitand hosts **14**–**16** as well as for trimers **3** and **4**. Although **3** and **4** do not have diastereotopic inter-bowl acetals and thus no dispersion, the chemical shift of these protons (especially bound versus free) gives some indication of their preferred conformation. Tris-cyanobenzyl **16** is easier to purify than **15**, and its electron-deficient arenes affect its binding properties (see below).

It is evident from the data in Table 11 that all hosts prefer conformation **A** in $CDCl_3$ (or $CHCl_3/CD_3OD$). **A** is also preferred by tris-hydroxy **14** in [D_5]nitrobenzene, whereas tris-benzyl **15** and tris-cyanobenzyl **16** prefer **B**/**C** in [D_5]nitrobenzene as well as in [D_8]toluene. Hexabenzyl trimer **3** also prefers conformations **B**/**C** in [D_5]nitrobenzene, [D_8]toluene, and C_6D_6. Binding of tris-acetylene **6** to **15** or **16** in [D_5]nitrobenzene or [D_8]toluene shifts the equilibrium from **B**/**C** toward conformation **A**, and binding of **6** to **14** appears to push the conformation further to **A**.[22] Likewise, binding of **6** to **3** or **4** appears to shift the conformation toward **A**. These data suggest that $CDCl_3$ binds more strongly to the hosts than does nitrobenzene. Thus $CDCl_3$ promotes conformation **A** and weakens binding of **6** through competition. In the absence of a good binder (e.g., in [D_5]nitrobenzene), the conformations of the hosts favor **B**/**C**. CPK models suggest that these conformations create a smaller cavity where exposed surfaces are minimized. The benzyl groups of **3**, **15**, and **16** may also partially fill the cavities of these hosts in less competitive solvents. In the presence of a suitable guest, the benzyl groups and acetals flip out and create a larger, more accommodating binding cavity.

Temperature also has an effect on the conformations of hosts **15** and **16** in [D_5]nitrobenzene (Table 12). The chemical shifts move downfield with increasing temperature with both hosts, and the dispersion is greatly reduced. Thus conformation **A** is favored at higher temperatures, which indicates that entropy disfavors conformations **B**/**C**. This may be due to the entropic cost of self-complexation of benzyl groups in conformations **B**/**C**.

Stability constants were determined for the three trimer cavitands using tris-acetylene **6** as guest in [D_5]nitrobenzene (Table 13). Tris-benzyl **15** gave the strongest complex, so K_s values were also determined between **15** and guests **9** and **7** (Table 13). The trimer cavitand complexes are significantly weaker than the complexes of trimer **3**. This may be due to repulsive interactions between the electron rich guest **6** with the moderately electron rich cap, or it may be an entropic problem, as the trimer cavitands restrict the guest more

Table 12. ^{1}H NMR data for trimer cavitands **15** and **16** at various temperatures in [D_5]nitrobenzene.

Trimer cavitand	T [K]	δ (ppm)	$\Delta\delta$ (ppm)
15	300	5.07, 5.81	0.74
	325	5.39, 5.86	0.47
	350	5.68, 5.89	0.21
	375	5.86, 5.92	0.06
	385	5.91, 5.91	0.00
16	300	5.09, 5.85	0.76
	350	5.64, 5.90	0.26
	400	5.90, 5.90	0.00

Table 13. Stability constants for trimer cavitand complexes with various guests ([D_5]nitrobenzene, 300 K).

Host	Guest	K_s [M^{-1}]
tris-cyanobenzyl **16**	**6**	250
tris-hydroxyl **14**	**6**	200
tris-benzyl **15**	**6**	1200
tris-benzyl **15**	**9**	3
tris-benzyl **15**	**7**	2–9*

[*] The tris-ester was observed to form two different complexed species. Therefore a range is reported based on K_s values estimated for each of the two different species.

Table 11. ^{1}H NMR chemical shift data for acetal protons of A,C-trimer derivatives and their complexes with **6** at 300 K.

Host	Solvent	δ (free)	$\Delta\delta$ (free)	δ (bound)*	$\Delta\delta$ (bound)*	$\Delta\delta$ (free-bound)*
3	$CDCl_3$	5.60	0.00	5.75	0.00	−0.15
	CD_2Cl_2	5.58	0.00	5.73	0.00	−0.15
	C_6D_6	5.33	0.00	5.90	0.00	−0.57
	[D_8]toluene	5.27	0.00	5.87	0.00	−0.67
	[D_5]nitrobenzene	5.58	0.00	6.15	0.00	0.57
4	$CDCl_3$:CD_3OD (19:1)	5.72	0.00	5.84	0.00	−0.12
14	$CDCl_3$	5.85/5.71	0.14	–	–	–
	[D_5]nitrobenzene	6.02/5.94	0.08	6.22/6.15	0.07	−0.28/−0.21[a]
15	$CDCl_3$	5.81/5.68	0.13	–	–	–
	[D_5]nitrobenzene	5.81/5.02	0.79	6.17/6.05	0.12	−1.15/−1.03[a]
	[D_8]toluene	5.55/4.54	1.01	–	–	–
16	$CDCl_3$	5.82/5.72	0.10	–	–	–
	[D_5]nitrobenzene	5.85/5.09	0.76	6.18/6.10	0.08	−1.09/−1.01[a]
	[D_8]toluene	5.60/4.74	0.86	–	–	–

[*] Bound refers to complexes between the respective hosts and tris-acetylene **6**. [a] Since the diastereotopic protons could not be unambiguously assigned, the two $\Delta\delta$ values are upper and lower limits.

severely than do the uncapped trimers. Since the trimer cavitands are weak binders of guests, they could not be used effectively as transition-state models. Thus no comparison can be made between the trimer cavitands and the other hosts in this regard.

We wondered if the single opening in the trimer cavitands versus the two openings of the uncapped trimers would affect the rate of guest entry. Could this restriction be the cause for the weaker binding? Thus, for complexes **3·6** and **15·6**, decomplexation rate constants, k_d, were measured by 1D EXSY, and complexation rate constants, k_c, were calculated from $K_s = k_c/k_d$; activation free energies of complexation ($\Delta G_c^{\neq}$) and decomplexation ($\Delta G_d^{\neq}$) were also calculated (Table 14).[23] The decomplexation rates are similar, but the complexation rate is much faster for **3·6** than for **15·6**. Thus, the weak binding in the trimer cavitands results from slow complexation. Apparently, a guest must "wait" for solvent to leave before it can enter the single entry port of trimer cavitand **15**, whereas displacement is facile with trimer **3** as there is both an entry and an exit port. Regarding decomplexation, the restriction of the single portal in **15** likely slows decomplexation, but this is compensated by its intrinsically weaker binding with respect to **3**, thus equalizing the two decomplexation rates.

Binding studies using host **17** and guest **6** were also conducted. The low symmetry of **17** allows two bound acetylene protons to be observed, which demonstrates that rotation of this guest inside **17**, and likely inside all the trimer hosts, including carceplex **5·6**, is slow. Coalescence of these signals yields a value for $\Delta G_{330}^{\neq} = 16.4$ kcal mol^{-1} ($\Delta\nu =$ 39.0 Hz at 283 K). CPK models suggest that simple rotation of the guest about its C_3 axis is prohibitive due to its snug fit within the host. It most likely tilts out of the plane perpendicular to the host's C_3 axis to rotate via a wobble. K_s for **17·6** was determined to be 40 M, which is very weak compared with hosts **3** and **15**. This weak binding is likely due to similar reasons for **15** binding more weakly than **3**. Both complexation and decomplexation are slow for **17**, as reflected by the weak binding and the relative guest exchange rates: **17·6** takes 30 minutes to reach equilibrium at 300 K (cf. Table 14). Weak binding of guests by **17** precludes full analysis of **17** as a transition-state model. Nevertheless, this relatively rapid guest exchange (with respect to the timescale of the reaction to form **5**) demonstrates that the GDS in formation of **5**·guest(s) is formation of the final C–O bond of the second cap.

Restricted motion as well as restricted guest conformational interconversions were also observed inside carceplex **5·7**. In ^{1}H NMR spectra at 250 K in $CDCl_3$, the intra-bowl acetals are split into two sets of equal intensity, while the para H are split into two sets in a ratio of 2:1 (Figure 3). Each ester

Table 14. Activation free energy of complexation ($\Delta_c^{\neq}$) and decomplexation ($\Delta G_d^{\neq}$), stability (K_s) and rate (k_c, k_d) constants for complexes **3·6** and **15·6** ([D$_5$]nitrobenzene, 330 K).

Host	K_s [M^{-1}]	k_c [M^{-1}s^{-1}]	$\Delta G_c^{\neq}$ [kcal mol^{-1}]	k_d [s^{-1}]	$\Delta G_d^{\neq}$ [kcal mol^{-1}]
3	21000	57000	12.2	2.7	18.7
15	1200	2600	14.2	2.2	18.9

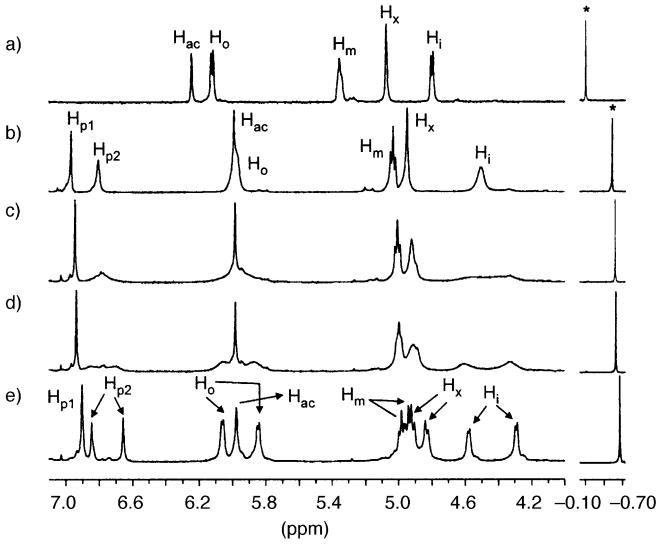

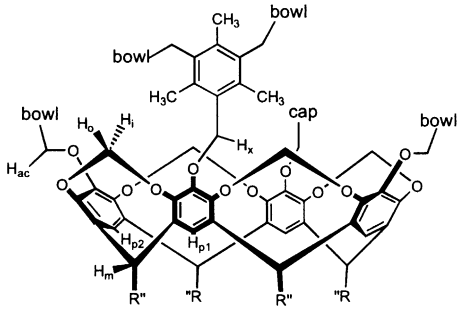

5: R" = $CH_2CH_2C_6H_5$

Figure 3. ^{1}H NMR spectra (500 MHz) of **5·7**. a) **5·7** in [D$_5$]nitrobenzene at 400 K and in $CDCl_3$ at b) 330 K, c) 300 K, d) 290 K, e) 250 K. * = CO_2CH_3 of **7**.

can exist in the *E* or *Z* form (the *Z* is usually favored and the energy barrier is only 1–2 kcal mol^{-1}),[24] and the carbonyls can either all be oriented in the same direction in the plane of the arene or one can be oriented in the opposite direction from the other two. The simplest situation is all three carbonyls being oriented in the same direction, and the conformations all being *Z* or rotating quickly. This is consistent with the observed spectra. Thus other conformations are either negligible, give coincident spectra, or in the case of the *E*/*Z* conformations are in fast exchange. 1D EXSY experiments on the two H_{in} intra-bowl acetal protons at 267 K in CD_2Cl_2 gave a rate constant of 13.0 s^{-1} ($\Delta G_{267}^{\neq} =$ 14.2 kcal mol^{-1}), which represents the rate of rotation of the esters about the Ar–CO bond. This energy barrier is about three times greater than for the corresponding rotation in methyl benzoate.[25] It appears that the three rotations must be concerted; a similar additive effect on conformational restriction was observed for the host in a disulfide-linked [5]carceplex.[14]

Reversible binding of multiple molecules to trimer hosts was also investigated. DMSO was used as guest due to its superior multi-molecule templating ability, and trimer **3** was used as host due to its strong binding properties. At 300 K in [D$_8$]toluene, a fast exchanging complex is evident, as the host signals shift, but large quantities of DMSO are needed for

such changes to occur. At 250 K, bound DMSO is observed at 0.43 ppm (free is at 1.67 ppm), which was confirmed by 1D NOESY. Likewise, bound host signals are observed. The ratio of bound host to bound guest is 1:3.5. This may correspond to 3.5 DMSO molecules per host, or an average of complexes. Although the binding of DMSO by **3** is weak, it is evident that hosts such as **3** can act as transition-state models, and potentially as screens, for the multi-molecule template effect in forming carceplexes or other containers.

Carceplex **5**·NFP·DMSO provides a probe for the mobility of multiple guests within a carceplex. At 200 K in CD_2Cl_2, two bound DMSO signals were observed, one at 0.69 ppm and one at -1.89 ppm. This huge dispersion indicates that one DMSO methyl is oriented deep within a bowl while the other is oriented toward the center of the cavity. The value for the activation energy was determined to be $\Delta G^{\ddagger}_{250} = 10.5\ \mathrm{kcal\,mol^{-1}}$ using coalescence measurements. This energy corresponds to removal of a methyl group from a bowl, either via rotation of DMSO within one bowl, or via movement from one bowl to another. The corresponding energy barrier for **5**·$(DMSO)_3$ is estimated to be $7.7\ \mathrm{kcal\,mol^{-1}}$ based on broad signals observed at 185 K and using the same $\Delta\nu$ (1032 Hz) from **5**·NFP·DMSO. Energy barriers for rotation of DMSO within a two bowl carceplex was reported to be $12.7\ \mathrm{kcal\,mol^{-1}}$.[26] There appears to be more room for movement in the present case, especially with three small guest molecules versus one small and one medium sized guest molecule.

We discovered something new with carceplex **5**·guest(s), reversible binding of water. In nearly all cases, ^{1}H NMR spectra of **5**·guest(s) manifested multiple host and guest signals that are in slow exchange. Signals corresponding to bound water are often observed as well. By recording the spectra in the presence of crushed 4 Å molecular sieves the "dry" host predominates, while recording spectra in water-saturated solvent yields more of the "wet" species. Carceplexes and hemicarceplexes have not been shown to bind water along with other guests. Table 15 lists the ^{1}H NMR chemical shifts of bound waters in carceplex **5**·guest(s). The dispersion is huge and indicates that water can sit in vastly different parts of the carceplex, depending on the occupation of the co-habiting guest(s). Presumably, the extent of binding of water to the incarcerated guest(s) also affects the chemical shift of the bound water. No evidence was observed for binding of water to **5**·$(DMF)_3$. Exchange rates are typically on the order of minutes; the solutions reach equilibrium as soon as the spectra are taken, and only weak EXSY correlations can be observed at ambient temperatures (heating the samples shifts the equilibrium toward the dry species, which precludes rate measurements). Carceplex **5**·$(DMSO)_3$ is anomalous in that two major bound DMSO species are observed, but no bound water was found. Either free and bound water have coincident chemical shifts or the two species differ by several waters, such that single waters exchange quickly (and are averaged with the observed "free" signal), but the two carceplex species do not. Figure 4 shows ^{1}H NMR spectra of **5**·$(DMA)_2$ under various conditions, demonstrating at least two hydrated species. These spectra, combined with NOESY data, show that one of the hydrates

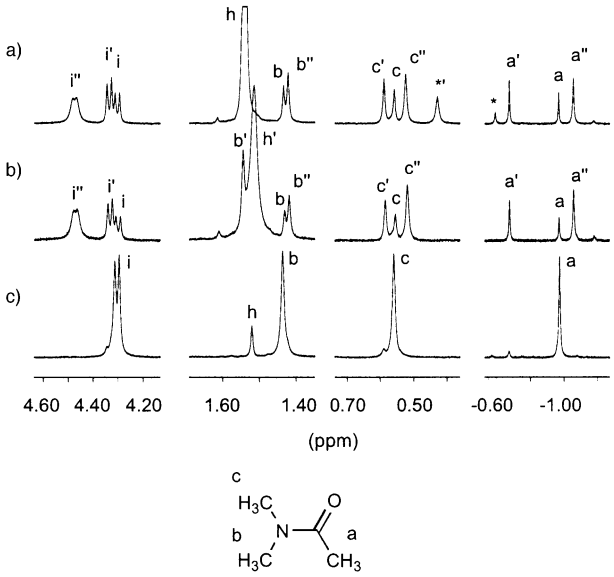

Figure 4. Expanded regions of ^{1}H NMR spectra (400 MHz) of **5**·$(DMA)_2$. a) H_2O-saturated $CDCl_3$; b) D_2O-saturated $CDCl_3$, and c) sieve-dried $CDCl_3$. a, b, c, and i (H_i) are for **5**·$(DMA)_2$. a′, b′, c′, i′ (H_i'), and * (bound H_2O) are for **5**·$(DMA)_2$·H_2O. a″, b″, c″, i″ (H_i''), and *′ (bound H_2O) are for **56**·$(DMA)_2$·$(H_2O)_2$. h = free H_2O. h′ = free HDO.

contains one water (-0.59 ppm), and the other two waters (0.43 ppm). The equilibrium constants for binding these waters are 25 and $11\,\mathrm{M^{-1}}$. Carceplex **13**·$(DMA)_2$, which has no methyls in the caps, manifests broad ^{1}H NMR spectra, which sharpen upon heating or drying. This suggests that this carceplex also binds water, but that exchange of waters is much faster, as one would expect. A final note is that addition of TFA to **5**·$(DMA)_2$·$(H_2O)_x$ in water-saturated C_6D_6 reduces the amount of hydrate. Addition of DBU has a similar, but less dramatic effect (Figure 5). Apparently, the water is needed in solution to solvate these polar species, so the equilibrium is shifted toward water removal from the cavity. These results will have important ramifications for reactions inside the trimer carceplex, to be reported shortly.

Conclusions

Multiple molecules can be used as templates in the formation of a carceplex. Competition between guests of different molecularity is possible. Multiple molecules suffer a larger entropic cost, at least in the system presented here. Expectation is that very large systems would manifest low selectivity toward multiple molecule templates, as micro-homogeneous fluids would have to form in solution. In such cases a template effect and a solvent effect would be indistinguishable. Such large systems remain as a challenge to construct.

Transition-state models for the formation of **5**·guest were also constructed. Hosts that appear to better resemble the transition state of the GDS manifested weaker binding, thus limiting exploration of their transition-state model properties. Nevertheless, models have been generated that can act as

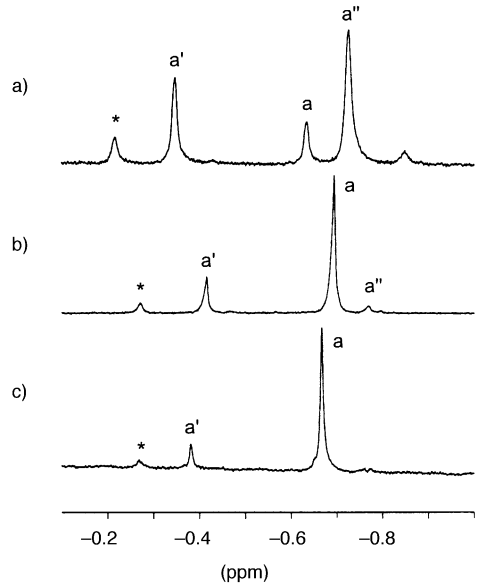

Figure 5. ^{1}H NMR spectra (500 MHz, H_2O-saturated C_6D_6) of the acetyl methyl protons of **5**·$(DMA)_2$·$(H_2O)_y$. a) **5**·$(DMA)_2$·$(H_2O)_y$. b) **5**·$(DMA)_2$·$(H_2O)_y$ and 180 mM TFA (5 equiv per H_2O). c) **5**·$(DMA)_2$·$(H_2O)_y$ and 670 mM DBU (20 equiv per H_2O). * = bound H_2O. a = **5**·$(DMA)_2$. a′ = **5**·$(DMA)_2$·H_2O. a″ = **5**·$(DMA)_2$·$(H_2O)_2$.

Table 15. ^{1}H NMR chemical shift data for bound H_2O in carceplexes **5**·guests·$(H_2O)_y$ in $CDCl_3$ at 300 K.

Guest(s)	δ_{bound} (H_2O)[a]	$\Delta\delta$ $(\delta_{free} - \delta_{bound})$[b]
hexanophenone	0.61, −1.24	0.93, 2.78
butyrophenone	0.73, −0.43, −1.57	0.81, 1.97, 3.11
1,3,5-tris(ethynyl)benzene	−0.20	1.74, 2.84
trimethyl 1,3,5-benzenetricarboxylate	−0.14, −0.80	1.68, 2.34
1,3,5-trimethoxybenzene	0.61, 0.11, −0.11	1.43, 1.65, 2.15
1,3,5-triethylbenzene	1.03, 0.65, −1.00	0.51, 0.89, 2.54
NFP	0.60, 0.10, −0.78, −1.72	0.94, 1.44, 2.32, 3.26
NFP·DMSO	0.64, 0.61, −0.24, −1.48	0.90, 0.93, 1.78, 3.02
$(NMP)_2$	0.47, −0.98	1.07, 2.52
$(DMA)_2$	0.43, −0.59	1.11, 2.13

[a] In H_2O saturated $CDCl_3$. [b] δ_{free} (H_2O) in $CDCl_3$ is taken to be 1.54 ppm (relative to the residual C*H*Cl_3 signal at 7.24 ppm).

screens for new templates. Such an approach could facilitate the creation of new carceplexes or other containers. The best guest/template has complementary shape to the host and binds tightly inside transition-state models, and thus, presumably to the transition state. Like the prototypical carceplex template system,[4] the larger and better templates have highly restricted motion inside. The guest exchange rates in the complexes suggest that the GDS is formation of the final C–O bond of the second cap. Since the guest recognition by the models is similar to the template ratios, the rate constants for forming the final C–O bonds are likely to be very similar. The effect of the template is largely to increase the concentration of the key species immediately prior to the GDS.

The mobility of both hosts and entrapped guests suggests that there is some restricted motion and that the host can adjust its conformation somewhat to complement the guest. Finally, water can bind reversibly to carceplexes that contain permanently entrapped guests. The effect of bound water on entrapped species is of current interest.

Acknowledgement

We thank NSERC, NIH, and PRF for funding. We thank Christoph Naumann for optimizing formation of diol **2**, and Rajesh Mungaroo for helpful discussions on partial de-capping of **5**·guests(s).

[1] D. J. Cram, J. M. Cram, *Container Compounds and Their Guests*, The Royal Society of Chemistry, Cambridge, **1994**.
[2] K. Akiyama, Y. Zhao; K. Sueki, K. Tsukada, H. Haba, Y. Nagame, T. Kodama, S. Suzuki, T. Ohtsuki, M. Sakaguchi, K. Kikuchi, M. Katada, H. Nakahara, *J. Am. Chem. Soc.* **2001**, *123*, 181–182.
[3] R. K. Rana, A. Gedanken, *J. Phys. Chem. B* **2002**, *106*, 9769–9776.
[4] a) R. G. Chapman, J. C. Sherman, *J. Org. Chem.* **1998**, *63*, 4103–4110; b) D. A. Makeiff, D. J. Pope, J. C. Sherman, *J. Am. Chem. Soc.* **2000**, *122*, 1337–1342.
[5] a) J. Kang, J. Rebek, Jr., *Nature* **1996**, *382*, 239–241; b) R. Meissner, X. Garcias, S. Mecozzi, J. Rebek, Jr., *J. Am. Chem. Soc.* **1997**, *119*, 77–85; c) J. Kang, G. Hilmersson, J. Santamaría, J. Rebek, Jr., *J. Am. Chem. Soc.* **1998**, *120*, 3650–3656.
[6] a) J. Kang, J. Rebek, Jr., *Nature* **1997**, *385*, 50–52; b) J. Kang, J. Santamaría, G. Hilmersson, J. Rebek, Jr., *J. Am. Chem. Soc.* **1998**, *120*, 7389–7390; for Diels–Alder reactants in a non-softball capsule, see T. Ooi, Y. Kondo, K. Maruoka, *Angew. Chem.* **1998**, 110, 3213–3215; *Angew. Chem. Int. Ed.* **1998**, *37*, 3039–3041.
[7] a) T. Heinz, D. M. Rudkevich, J. Rebek, Jr., *Angew. Chem.* **1999**, 111, 1206–1209; *Angew. Chem. Int. Ed.* **1999**, *38*, 1136–1139; b) S. K. Körner, F. C. Tucci, D. M. Rudkevich, T. Heinz, J. Rebek, Jr., *Chem. Eur. J.* **2000**, *6*, 187–195; c) J. Chen, J. Rebek, Jr., *Org. Lett.* **2002**, *4*, 327–329; d) J. Chen, S. Körner, S. L. Craig, D. M. Rudkevich, J. Rebek, Jr., *Nature* **2002**, *415*, 385–386; e) J. Chen, S. Körner, S. L. Craig, S. Lin, D. M. Rudkevich, J. Rebek, Jr., *Proc. Nat. Acad. Sci.* **2002**, *99*, 2593–2596.
[8] a) T. Kusukawa, M. Fujita, *J. Am. Chem. Soc.* **1999**, *121*, 1397–1398; b) T. Kusukawa, M. Yoshizawa, M. Fujita, *Angew. Chem.* **2001**, *113*, 1931–1936; *Angew. Chem. Int. Ed.* **2001**, *40*, 1879–1884.
[9] M. Yoshizawa, T. Kusukawa, M. Fujita, K. Yamaguchi, *J. Am. Chem. Soc.* **2000**, *122*, 6311–6312.
[10] S.-Y. Yu, T. Kusukawa, K. Birada, M. Fujita, *J. Am. Chem. Soc.* **2000**, *122*, 2665–2666.
[11] a) L. R. MacGillvray, J. L. Atwood, *Nature* **1997**, *389*, 469–472; b) T. Gerkensmeier, W. Iwanek, C. Agena, R. Fröhlich, S. Kotila, C. Näther, J. Mattay, *Eur. J. Org. Chem.* **1999**, 2257–2262; c) J. L. Atwood, L. J. Barbour, A. Jerga, *Chem. Commun.* **2001**, 2376–2377; d) A. Shivanyuk, J. Rebek, Jr., *Proc. Nat. Acad. Sci.* **2001**, *98*, 7662–7665; e) A. Shivanyuk, J. Rebek, Jr., *Chem. Commun.* **2001**, 2424–2425; f) A. Shivanyuk, J. Rebek, Jr., *Chem. Commun.* **2001**, 2374–2375; g) J. L. Atwood, L. J. Barbour, A. Jerga, *Proc. Nat. Acad. Sci.* **2002**, *99*, 4837–4841; h) L. Avram, Y. Cohen, *J. Am. Chem. Soc.* **2002**, *124*, 15148–15149; i) L. Avram, Y. Cohen, *Org. Lett.* **2002**, *4*, 4365–4368.
[12] a) J. A. Bryant, M. T. Blanda, M. Vincenti, D. J. Cram, *J. Chem. Soc. Chem. Commun.* **1990**, 1403–1405; b) J. A. Bryant, M. T. Blanda, M. Vincenti, D. J. Cram, *J. Am. Chem. Soc.* **1991**, *113*, 2167–2172.
[13] D. J. Cram, M. E. Tanner, C. B. Knobler, *J. Am. Chem. Soc.* **1991**, *113*, 7717–7727.
[14] C. Naumann, S. Place, J. C. Sherman, *J. Am. Chem. Soc.* **2002**, *124*, 16–17.
[15] N. Chopra, J. C. Sherman, *Angew. Chem.* **1999**, *111*, 2109–2111; *Angew. Chem. Int. Ed.* **1999**, *38*, 1955–1957.
[16] N. Chopra, Ph.D. thesis, University of British Columbia

[17] DMA, dimethylacetamide; NMP, *N*-methylpyrrolidinone; NFP, *N*-formylpiperidine (**10**); butyrophenone (**11**).
[18] S. X. Gui, J. C. Sherman, *J. Chem. Soc. Chem. Commun.* **2001**, 2680–2681.
[19] K. Nakamura, C. Sheu, A. E. Keating, K. N. Houk, J. C. Sherman, R. G. Chapman, W. L. Jorgensen, *J. Am. Chem. Soc.* **1997**, *119*, 4321–4322.
[20] R. G. Chapman, G. Olivsson, J. Trotter, J. C. Sherman, *J. Am. Chem. Soc.* **1998**, *120*, 6252–6260.
[21] A. Jasat, J. C. Sherman, *Chem. Rev.* **1999**, *99*, 931–967.
[22] The anisotropy of bound **6** would likely also cause a downfield shift in the host's inter-bowl acetals, but not a decrease in their $\Delta\delta$ which is most likely the result of a conformational change in the host.
[23] $\Delta G^{+} = -RT\ln(kh/k_{B}T)$
[24] a) E. L. Eliel, S. H. Wilen, *Stereochemistry of Organic Compounds*, Wiley, New York, **1994**, p. 618–619; b) D. C. Spellmeyer, P. D. J. Grootenhuis, M. D. Miller, L. G. Kuyper, P. A. Kollman, *J. Phys. Chem.* **1990**, *94*, 4483–4491.
[25] T. Drakenberg, J. Sommer, R. Jost, *J. Chem. Soc. Perkin 2* **1980**, 363.
[26] R. G. Chapman, J. C. Sherman, *J. Am. Chem. Soc.* **1999**, *121*, 1962–1963.

Received: January 28, 2003 [F4780]